The Plant Cell, Vol. 24: 676–691, February 2012, www.plantcell.org

PPR2263, a DYW-Subgroup Pentatricopeptide Repeat Protein, Is Required for Mitochondrial *nad5* and *cob* Transcript Editing, Mitochondrion Biogenesis, and Maize Growth [C][W]

Davide Sosso,[a,b,c,1] Sylvie Mbelo,[a,b,c] Vanessa Vernoud,[a,b,c] Ghislaine Gendrot,[a,b,c] Annick Dedieu,[a,b,c] Pierre Chambrier,[a,b,c] Myriam Dauzat,[d] Laure Heurtevin,[e] Virginie Guyon,[f] Mizuki Takenaka,[g] and Peter M. Rogowsky[a,b,c,2]

[a] University of Lyon, Ecole Normale Supérieure de Lyon, Université Lyon 1, Unité Reproduction et Développement des Plantes, F-69364 Lyon, France

[b] Institut National de la Recherche Agronomique, Unité Mixte de Recherche 879 Reproduction et Développement des Plantes, F-69364 Lyon, France

[c] Centre National de la Recherche Scientifique, Unité Mixte de Recherche 5667 Reproduction et Développement des Plantes, F-69364 Lyon, France

[d] Institut National de la Recherche Agronomique, Unité Mixte de Recherche 759 Ecophysiologie des Plantes sous Stress Environnementaux, F-34060 Montpellier, France

[e] Institut National de la Recherche Agronomique, Unité Mixte de Recherche 1165 Recherche en Génomique Végétale, F-91057 Evry, France

[f] Biogemma SAS, Cereals Genetics and Genomics, F-63720 Chappes, France

[g] Department of Molecular Botany, University of Ulm, D-89069 Ulm, Germany

RNA editing plays an important role in organelle gene expression in various organisms, including flowering plants, changing the nucleotide information at precise sites. Here, we present evidence that the maize (*Zea mays*) nuclear gene *Pentatricopeptide repeat 2263* (*PPR2263*) encoding a DYW domain–containing PPR protein is required for RNA editing in the mitochondrial *NADH dehydrogenase5* (*nad5*) and *cytochrome b* (*cob*) transcripts at the *nad5*-1550 and *cob*-908 sites, respectively. Its putative ortholog, *MITOCHONDRIAL EDITING FACTOR29*, fulfills the same role in *Arabidopsis thaliana*. Both the maize and the *Arabidopsis* proteins show preferential localization to mitochondria but are also detected in chloroplasts. In maize, the corresponding *ppr2263* mutation causes growth defects in kernels and seedlings. Embryo and endosperm growth are reduced, leading to the production of small but viable kernels. Mutant plants have narrower and shorter leaves, exhibit a strong delay in flowering time, and generally do not reach sexual maturity. Whereas mutant chloroplasts do not have major defects, mutant mitochondria lack complex III and are characterized by a compromised ultrastructure, increased transcript levels, and the induction of alternative oxidase. The results suggest that mitochondrial RNA editing at the *cob*-908 site is necessary for mitochondrion biogenesis, cell division, and plant growth in maize.

INTRODUCTION

One of the distinctive features of vascular plant genomes is the marked expansion of the pentatricopeptide repeat (PPR) family, with 450 members in *Arabidopsis thaliana* and 477 in rice (*Oryza sativa*) compared with 103 members in the moss *Physcomitrella patens*, six in humans (*Homo sapiens*), and two in *Drosophila melanogaster* (Lurin et al., 2004; O'Toole et al., 2008). The family is characterized by the PPR domain, a degenerate sequence of 35 amino acids characteristic of each family member that is repeated on average 12 times in the protein sequence. Although the three-dimensional structure of this motif has not been determined experimentally, in silico modeling guided by the crystal structure of the related tetratricopeptide repeat (TPR) domain (Das et al., 1998) suggests that the PPR motif is arranged in a pair of antiparallel α-helixes (Small and Peeters, 2000). In both the TPR and PPR domains, the repetition of numerous TPR/PPR motifs is thought to form a super-helix with a central groove that hosts the target molecule, protein in the case of the TPR domain (D'Andrea and Regan, 2003) or RNA in the case of the PPR domain (Delannoy et al., 2007). RNA binding of PPR proteins has been demonstrated by gel shift, cross-linking, and affinity assays (reviewed in Delannoy et al., 2007).

In *Arabidopsis*, PPR proteins have been divided into two classes of roughly equal size based on structural criteria. P-class proteins contain canonical PPR motifs (P-motifs, 35 amino acids) in tandem repeats, whereas PLS-class proteins are characterized by the presence of longer (L-motifs, 36 amino acids) and shorter (S-motifs, 31 amino acids) motifs forming tandemly repeated PLS triplets (Lurin et al., 2004). The PLS class

[1] Current address: Carnegie Institution for Science, 260 Panama St., Stanford, CA 94305.

[2] Address correspondence to peter.rogowsky@ens-lyon.fr.

The author responsible for distribution of materials integral to the findings presented in this article in accordance with the policy described in the Instructions for Authors (www.plantcell.org) is: Peter M. Rogowsky (peter.rogowsky@ens-lyon.fr).

[C] Some figures in this article are displayed in color online but in black and white in the print edition.

[W] Online version contains Web-only data.

www.plantcell.org/cgi/doi/10.1105/tpc.111.091074

is further subdivided into three subclasses on the basis of the successive addition of the E, E+, and DYW domain at the C terminus (Lurin et al., 2004). Independently of the subclass, three-quarters of the PPR proteins are predicted to be targeted to either mitochondria or chloroplasts, whereas no clear prediction is made for the rest. In addition to numerous experimental localizations in plastids and mitochondria, nuclear (Ding et al., 2006) or dual localization to mitochondria and nuclei (Hammani et al., 2011) has been demonstrated experimentally. Whereas PPR proteins have been implicated in a wide range of biological processes, including photosynthesis, pollen development, and embryogenesis, there seems to be a common underlying molecular function in the form of sequence-specific associations with RNA that govern various steps in RNA metabolism, such as cleavage, splicing, stability, editing, and translation (Schmitz-Linneweber and Small, 2008; Fujii and Small, 2011).

The term RNA editing describes a set of mechanisms that change the nucleotide sequence of an RNA molecule from that of the DNA template encoding it. It was first used to describe insertions and deletions of uridines in mitochondrial mRNAs of *Trypanosoma brucei* (Benne et al., 1986). Subsequently, its use was extended to describe posttranscriptional base substitutions in the mitochondrial mRNA of mammals (Powell et al., 1987) and plants (Covello and Gray, 1989). In plants, the modification of specific cytidines (C) to uridines (U) and the reverse U-to-C editing are limited to organelles, whereas adenosine (A) to inosine (I) modification also occurs in cytosolic tRNAs (Chateigner-Boutin and Small, 2010). Complex thalloid liverworts of the subclass *Marchantiidae* are the only examined land plants in which the editing of organellar transcripts has not been observed (Steinhauser et al., 1999). In the model species *Arabidopsis*, RNA editing affects 34 well-defined sites in chloroplasts (Chateigner-Boutin and Small, 2007) and ~450 sites in mitochondria with variations due to the methods and organs used (Giegé and Brennicke, 1999; Bentolila et al., 2008). Editing sites are only partially conserved, even between closely related species (Handa, 2003). In addition, RNA editing at a given site is not always complete, and the editing efficiency can vary between ecotypes (Zehrmann et al., 2008).

Whereas it is now commonly agreed that the specificity of the C-to-U editing is provided by PPR proteins that bind 10 to 25 nucleotides upstream of the C that will be edited (Okuda et al., 2006), the protein(s) responsible for the actual editing by cytidine deamination remains to be formally identified (Chateigner-Boutin and Small, 2010). The C-terminal DYW domain of the respective PPR proteins may possess catalytic editing activity as proposed initially by in silico analyses demonstrating a strict correlation of the phylogenetic distribution of the DYW domain and RNA editing as well as sequence similarities with cytidine deaminases (Salone et al., 2007; Rüdinger et al., 2008). Similarly, the E/E+ domain has been hypothesized to be involved in the binding of a nonidentified editing enzyme. These hypotheses have been corroborated subsequently by the fact that all of the over 30 editing mutants identified to date carry lesions in PPR proteins of the E/E+ or DYW class (Chateigner-Boutin and Small, 2010). However, exceptions seem to exist since the DYW domains of the plastid-located CRR22, CRR28, and OTP28 and of the mitochondrial factor MITOCHONDRIAL EDITING FACTOR11 (MEF11) are not essential for RNA editing in vivo (Okuda et al., 2009, 2010; Zehrmann et al., 2011) and since CRR2 and OTP70 belong to the DYW- and E-subclass, respectively, without being involved in RNA editing (Hashimoto et al., 2003; Chateigner-Boutin et al., 2011).

The maize (*Zea mays*) genome is estimated to harbor more than 450 *PPR* genes (Fujii and Small, 2011), and functional data exist for a few of them (Schmitz-Linneweber and Small, 2008). The majority of the characterized maize PPR proteins are targeted to plastids, such as Chloroplast RNA processing1 involved in translation (Schmitz-Linneweber et al., 2005), PPR2, PPR5, and PPR10 important for RNA stability (Williams and Barkan, 2003; Beick et al., 2008; Prikryl et al., 2011), and PPR4 and PPR5 responsible for RNA splicing (Schmitz-Linneweber et al., 2006; Williams-Carrier et al., 2008). The only functionally characterized PPR protein targeted to maize mitochondria is Empty Pericarp4 (Emp4) necessary for normal endosperm development. Although Emp4 has been shown to be required for the correct expression of a small group of mitochondrial genes, neither its mode of action nor its molecular target(s) is known (Gutiérrez-Marcos et al., 2007). So far no member of the RNA editing machinery in maize mitochondria or chloroplasts has been identified despite more than 400 edited sites (Takenaka et al., 2008; Fujii and Small, 2011).

Here, we report the phenotypic and molecular characterization of the *pentatricopeptide repeat2263* (*ppr2263*) mutant characterized by a reduced kernel size and a severely stunted vegetative apparatus. Transposon tagging and transgenic complementation demonstrate that a mutation in *PPR2263* coding for a PPR protein of the DYW subclass dually targeted to mitochondria and chloroplasts is responsible for the phenotype. PPR2263 and its ortholog MEF29 are required for RNA editing at the *nad5*-1550 and *cob*-908 sites in maize and *Arabidopsis*, respectively. The *ppr2263* mutant harbors mitochondria that lack complex III and have a compromised ultrastructure, generally increased transcript levels, and higher levels of alternative oxidase protein.

RESULTS

Phenotypic Characterization of the *ppr2263* Mutant

The *ppr2263* mutant was isolated in the course of a systematic forward genetics approach aimed at the cloning of 300 mutations responsible for kernel phenotypes in the *Mutator*-induced Biogemma mutant collection (Martin et al., 2006; Cossegal et al., 2008). The *ppr2263* mutation behaved as a monogenic recessive trait since the frequency of mutant kernels on segregating ears of self-pollinated heterozygote plants was on average 23.7% (Figure 1A). The observed reduction in kernel size involved both the embryo and endosperm (Figure 1B), and the seed was viable. A more detailed characterization during early kernel development was achieved by measurements of cytological sections and revealed that the sizes of both the embryo and the endosperm were greatly reduced at 9, 16, and 24 d after pollination (DAP; Table 1, Figure 1C).

Mutant kernels were not only smaller than wild-type kernels, they also showed a developmental delay. This was most evident for embryo development, which offered clear-cut morphological criteria. At 9 DAP, wild-type embryos had reached the coleoptilar stage characterized by clearly established bilateral symmetry, the separation of the scutellum from the embryo axis, and the

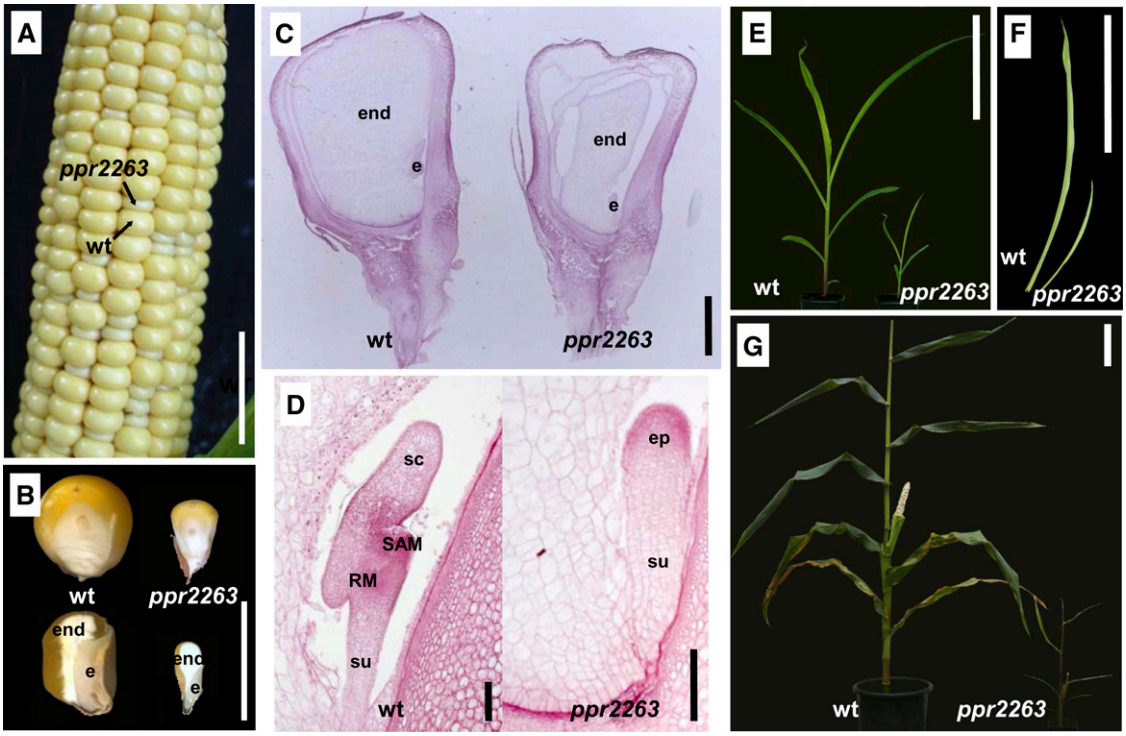

Figure 1. Kernel and Plant Phenotype of Mutant *ppr2263*.

(A) Maize ear segregating for the *ppr2263* mutation at 24 DAP. wt, wild type.
(B) Front view (top) or sagittal cut (bottom) of mature wild-type (left) or *ppr2263* (right) kernel.
(C) Schiff stain of sagittal cytological section of wild-type (left) or *ppr2263* (right) kernel at 9 DAP.
(D) Schiff stain of sagittal cytological section of wild-type (left) or *ppr2263* (right) embryo at 9 DAP.
(E) Wild-type (left) or *ppr2263* (right) seedlings at 21 DAS.
(F) Wild-type (left) or *ppr2263* (right) fully expanded leaf #5.
(G) Wild-type (left) or *ppr2263* (right) plant at sexual maturity.
e, embryo; end, endosperm, ep, embryo proper; RM, root meristem; SAM, shoot apical meristem; sc, scutellum; su, suspensor. Bars = 5 cm in **(A)**, 1 cm in **(B)**, 1 mm in **(C)**, 200 μm in **(D)**, and 20 cm in **(E)** to **(G)**.

formation of the shoot apical and the root meristem (Figure 1D). On the contrary, mutant embryos had just reached the transition stage, which marks the shift from radial to bilateral symmetry. There was no sign of the formation of the scutellum, the shoot apical meristem, or the root meristem (Figure 1D).

At maturity, *ppr2263* kernels had an average mass of only 0.08 g, which represented one-third of the average mass of wild-type kernels (Table 1). The germination frequency of *ppr2263* kernels was normal, but they took on average 2 d longer to germinate than did heterozygous or wild-type kernels from the same ear. The emerging *ppr2263* seedlings were reduced in size and their leaves were both shorter and narrower than those of the wild type (Figures 1E and 1F). In maize, leaf epidermal cells are arranged in parallel cell files along the proximal-distal axis. In the mutant, the number of cell files was reduced to half, both in the growing (bottom) and the elongation zone (middle) of the leaf blade (Table 1). By contrast, cell size was affected only in the growing zone, where a slight but significant reduction was observed in *ppr2263* leaves (Table 1). Taken together, these results indicate that the mutant seedlings are mainly affected in cell division rather than cell expansion.

The size difference between wild-type and *ppr2263* plants persisted and increased throughout vegetative development until flowering, which mutant plants reached with a delay of 35 d. At sexual maturity, there was a nearly threefold difference in plant height and a nearly twofold difference in leaf number between wild-type and mutant plants (Figure 1G, Table 1). In addition, the *ppr2263* plants carried a very small but well-formed ear with immature ovules and silks and very small tassels with poor, if any, pollen, rendering self-pollinations impossible.

Cosegregation between the *ppr2263* Phenotype and a *Mutator* Insertion in a *PPR* Gene

To isolate flanking sequences of the *Mutator* transposon responsible for the *ppr2263* phenotype, the novel MuExpress technique was used (see Methods and Supplemental Figure 1 online). The principal difference with classical transposon display methods, such as amplification of insertion mutagenized sites (AIMS) (Frey et al., 1998), thermal asymmetric interlaced (TAIL) PCR (McCarty et al., 2005), *Mutator* TAIL and AIMS (Yi et al., 2009), or

Table 1. Measurements of Vegetative and Reproductive Organs in Mutant *ppr2263*

Trait	Wild Type[a]	*ppr2263*	Significance[b]
Embryo length (9 DAP)	1.32 ± 0.06 mm	0.63 ± 0.08 mm	**
Embryo length (16 DAP)	1.72 ± 0.14 mm	1.09 ± 0.12 mm	**
Embryo length (24 DAP)	6.11 ± 0.70 mm	2.30 ± 0.30 mm	**
Endosperm surface (9 DAP)	10.7 ± 0.4 mm^2	3.8 ± 0.4 mm^2	**
Endosperm surface (16 DAP)	31.7 ± 2.7 mm^2	23.0 ± 0.8 mm^2	**
Endosperm surface (24 DAP)	62.7 ± 7.5 mm^2	34.1 ± 4.2 mm^2	**
Kernel mass (maturity)	243 ± 13 mg	89 ± 13 mg	**
Leaf epidermal cell file number (bottom)[c]	451 ± 34	204 ± 24	**
Leaf epidermal cell file number (middle)[c]	819 ± 84	429 ± 47	**
Leaf epidermal cell surface (bottom)[c]	2596 ± 571 μm^2	2080 ± 589 μm^2	**
Leaf epidermal cell surface (middle)[c]	1991 ± 428 μm^2	2107 ± 383 μm^2	
Flowering time	56 ± 0.9 DAS	91 ± 4.1 DAS	**
Plant height (sexual maturity)	185 ± 6 cm	66 ± 2 cm	**
Leaf number (sexual maturity)	14 ± 0.5	8 ± 0.5	**

[a]Value ± SD.
[b]Student's *t* test: **P value < 0.01; P value > 0.05.
[c]Fully expanded leaf #3 harvested from the wild type at 14 DAS and from *ppr2263* mutant at 24 DAS.

digestion-ligation-amplification (DLA) (Liu et al., 2009), was the use of cDNA rather than genomic DNA for the display, which captured only genes expressed in the kernel and consequently diminished the number of bands displayed. The nested 5′ rapid amplification of cDNA ends (RACE) reaction on 13-DAP kernel cDNA yielded a candidate band of ~800 bp that was present only in two independent *ppr2263* mutant samples but not in the corresponding wild-type sample (see Supplemental Figure 1 online). This band was cloned and sequenced. Alignment of the 681-bp *Mutator* flanking region with the maize genome placed the insertion unambiguously on the top of chromosome 9 in the middle of the intronless gene model AC215198.3_FG002 (Figure 2A). BLAST analysis of the deduced amino acid sequence revealed high similarity to the conserved domains pfam01535 and TIGR00756, classifying the encoded protein as a member of the PPR domain family. The underlying gene will be called *PPR2263* hereafter.

To establish a genetic link between the *ppr2263* phenotype and the *Mutator* insertion in *PPR2263*, cosegregation analysis was undertaken. A total of 142 small (*ppr2263*) and normally sized kernels were germinated and the resulting plants were phenotyped and genotyped with primers PPR2263-4F and PPR2263-4R flanking the *Mutator* insertion (Figure 2A), both as a pair and in combination with a primer in the terminal repeat of *Mutator*. The phenotypic evaluation demonstrated that all plants originating from *ppr2263* seeds not only showed strongly retarded growth but also were homozygous for the insertion. After self-pollination of the remaining plants, a perfect correlation was observed between heterozygosity for the insertion and the presence of approximately one-quarter small kernels on selfed ears on the one hand and the absence of the insertion and fully normal ears on the other. These data established a close genetic link between the *ppr2263* phenotype and the *Mutator* insertion in *PPR2263*.

Complementation of the *ppr2263* Mutation with a *PPR2263* Transgene

Since our attempts to find independent alleles in maize mutant collections were not successful, we decided to complement the *ppr2263* mutant with a transgenic construct to obtain proof that the mutation in *PPR2263* was indeed responsible for the *ppr2263* phenotype. To this end, the entire coding sequence was amplified from genomic DNA and placed under the control of the constitutive rice *Actin1* promoter (McElroy et al., 1990). Since the mutation was not in a genetic background that can be easily transformed (F252), we transformed the inbred line A188 and then pollinated single copy T0 plants with pollen from heterozygous +/*ppr2263* plants with F252 background. T1 plants were genotyped to identify individuals hemizygous for the *PPR2263* transgene and heterozygous for the *Mutator* insertion in *PPR2263*, the latter serving as a marker for the *ppr2263* mutation. Self-pollinated ears of double heterozygotes were analyzed for the frequency of small kernels to distinguish complementation (1/16 small) from absence of complementation (1/4 small). At 5.7% ± 1.9%, the frequency of small kernels was much closer to the 1:16 (6.25%) ratio expected in the case of complementation than to the 1:4 (25%) ratio expected otherwise.

To assure that not only the kernel phenotype but also the vegetative phenotype was complemented, 50 randomly chosen kernels from three complemented ears were germinated and the resulting seedlings analyzed for their genotype and phenotype. All plants carrying the transgene and homozygous for the *Mutator* insertion in *PPR2263* exhibited normal morphology and size, demonstrating complementation of the reduced growth phenotype. Taken together, all these results provided convincing evidence that the *Mutator* insertion in *PPR2263* was indeed responsible for the *ppr2263* mutant phenotype.

PPR2263, a Member of the DYW Subclass

PPR2263 encodes a predicted protein of 787 amino acids. Analysis of the 13 PPR domains guided by the annotation of the *Arabidopsis* and rice orthologs in FlagDB (http://urgv.evry.inra.fr/projects/FLAGdb++/HTML/index.shtml) revealed an alternation of canonical (P), long (L), and short (S) PPR domains and assigned PPR2263 to the PLS family (Lurin et al., 2004). Moreover, the C terminus of PPR2263, which is highly conserved

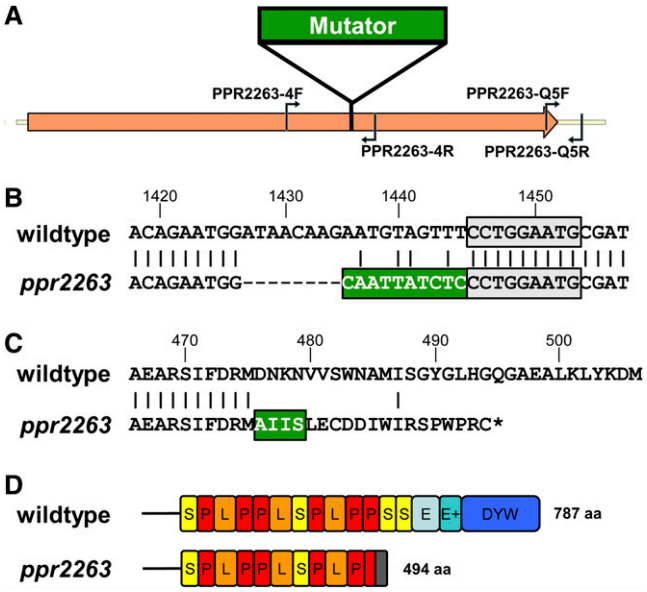

Figure 2. Molecular Characterization and Domain Composition of *PPR2263*.

(A) Schematic drawing of the intronless *PPR2263* gene indicating the position of the *Mutator* insertion in *ppr2263* and of primers used for genotyping and qRT-PCR.
(B) Alignment of wild-type and mutant cDNA sequences around the *Mutator* insertion point highlighting the replacement of 18 bp of native cDNA by 10 bp of *Mutator*-derived sequence (white lettering). The 9 bp duplicated upon *Mutator* insertion are marked with a box (black letters).
(C) Alignment of wild-type and mutant amino acid sequences around the *Mutator* insertion point pinpointing the frameshift caused by the insertion of *Mutator*-derived sequence (white lettering) resulting in a premature stop codon.
(D) Schematic diagram and comparison of domain composition between wild-type and mutant PPR2263 proteins. The mutant PPR2263 is truncated in the sixth P-domain. L, PPR long motif; P, PPR P-motif; S, PPR short motif; the E, E+, and DYW domains are also indicated in the diagram. aa, amino acids.
[See online article for color version of this figure.]

compared with its putative *Arabidopsis* (At4g30700) and rice orthologs (Os06g08600), contains an E, an E+, and a DYW domain (Figure 2D; see Supplemental Figure 2 online).

In the *ppr2263* mutant, PPR2263 was predicted to be truncated in the sixth P domain (Figure 2D). This prediction was based on nucleotide sequence analysis of mutant leaf cDNA, which suggested a noncanonical splicing event eliminating 18 nucleotides of *PPR2263* and adding 10 nucleotides of *Mutator* to the mature transcript (Figure 2B). The consequence at the protein level was not only the insertion of *Mutator* derived residues but, more importantly, a frameshift introducing a premature STOP codon (Figure 2C). Consequently, the mutant PPR2263 protein lacked not only three PPR domains but also the terminal E, E+, and DYW domains (Figure 2D), likely rendering the mutant protein nonfunctional.

Constitutive Expression of *PPR2263*

Despite the wealth of EST data available for maize (Messing and Dooner, 2006), none corresponded to *PPR2263*, in contrast with rice where a full-length cDNA (accession number AK120685) covered the entire sequence of the ortholog Os06g08660. To provide evidence for active transcription of *PPR2263*, quantitative RT-PCR (qRT-PCR) experiments with gene-specific primers (see Supplemental Table 1 online) were performed on major organs of the maize plant and during kernel development (Figure 3). *PPR2263* was expressed at very low levels in all vegetative and reproductive maize organs tested. Relative mRNA levels were highest in immature and mature ears, intermediate in juvenile leaf sheaths, seedlings, tassels, silks, and kernels and weak in leaves, roots, and stem (Figure 3A). *PPR2263* was also expressed in unfertilized ovaries and during all stages of kernel development from 1 to 70 DAP, with a peak at 9 DAP and the lowest expression at 15 DAP (Figure 3B). In the light of the very low overall expression level, the biological relevance of the observed variations was probably not very high, leading to the conclusion of a ubiquitous expression pattern of *PPR2263* consistent with a basic cellular function, such as RNA editing in organelles.

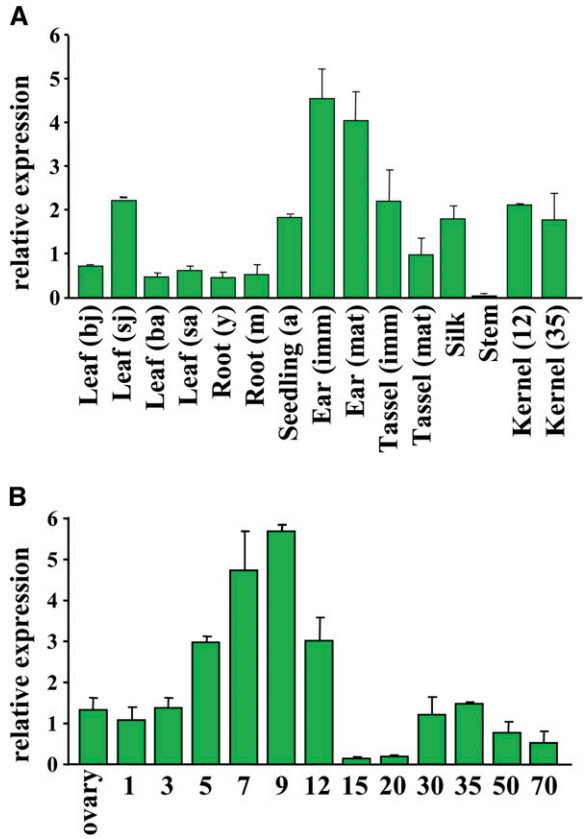

Figure 3. Expression Pattern of *PPR2263*.

(A) Relative expression levels of *PPR2263* in the maize organs indicated. 12, 12 DAP; 35, 35 DAP; a, aerial parts; ba, blade adult; bj, blade juvenile; imm, immature; m, mature; mat, mature; sa, sheath adult; sj, sheath juvenile; y, young.
(B) Relative expression levels of *PPR2263* during maize kernel development on a time scale in DAP.
qRT-PCR values for *PPR2263* are means of three technical replicates normalized with the *18S* gene. Error bars represent the SD.
[See online article for color version of this figure.]

Dual Targeting of PPR2263 to Mitochondria and Chloroplasts

To obtain predictions for the subcellular localization of PPR2263, we used the Predotar (Small et al., 2004) and TargetP (Emanuelsson et al., 2000) tools. In contrast with many other members of the PPR domain superfamily, the probability for localization in mitochondria (0.01/0.34 with Predotar/TargetP) or plastids (0.00/0.18) was lower than for other parts of the cell (0.95/0.58). Use of the SignalP tool (Emanuelsson et al., 2007) resulted in low signal peptide cleavage probability and conflicting cleavage site predictions by neural networks (after position 30) and hidden Markov models (after position 58).

To obtain experimental evidence of the subcellular localization of PPR2263, we generated a translational fusion of the full-length *PPR2263* cDNA with the green fluorescent protein (*GFP*) reporter gene under the control of the *35S* promoter, which was used for transient expression studies in *Nicotiana benthamiana* leaves via infiltration with *Agrobacterium tumefaciens*. To unequivocally identify mitochondria, the leaves were coinfiltrated with an *FDH*:red fluorescent protein (*RFP*) marker construct carrying a translational fusion of the mitochondrion-located formate dehydrogenase from potato (*Solanum tuberosum*; Ambard-Bretteville et al., 2003). Confocal laser scanning microscopy demonstrated colocalization of the green fluorescent signal of PPR2263:GFP both with the red mitochondrial signal of FDH:RFP and the autofluorescent signal of chloroplasts (Figures 4A to 4D). It should be noted that the green signal intensity was generally stronger in mitochondria than in chloroplasts and that in many cells only mitochondria, but not chloroplasts, produced green fluorescence.

Dual localization in mitochondria and chloroplasts was also observed for the putative *Arabidopsis* ortholog At4g30700. Translational fusions of the *RFP* reporter gene to the first 300 bp of the coding sequence or the full-length cDNA both led to fluorescence in mitochondria and in plastids of *Agrobacterium*-infiltrated *N. benthamiana* protoplasts (Figures 4E to 4H). In conclusion, both PPR2263 and its *Arabidopsis* ortholog showed dual localization with a preference for mitochondria.

Loss of *nad5*-1550 Editing in *ppr2263* and *mef29-1*

Guided by the hypothesis that many if not all PPR proteins of the DYW subgroup play a role in RNA editing (Salone et al., 2007), we set out to test if PPR2263 was involved in organelle RNA editing. Since the SNaPshot assay, a multiplexed single nucleotide extension protocol (Takenaka and Brennicke, 2009), was available only for *Arabidopsis*, we obtained homozygous plants from the SALK_096438 (BN) line that carries a T-DNA insertion in the coding sequence of the intronless gene At4g30700, the putative *Arabidopsis* ortholog of *PPR2263*. RNA editing was investigated at 383 individual sites in mitochondria and revealed a complete

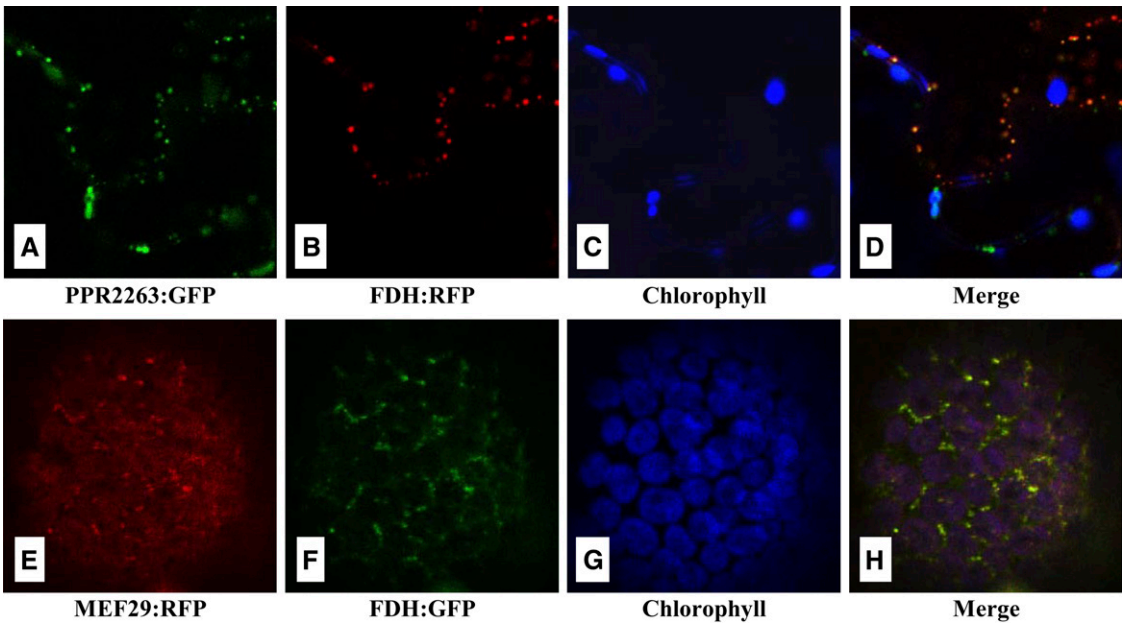

Figure 4. Subcellular Localization of Maize PPR2263 and *Arabidopsis* MEF29.

Transient expression in *Agrobacterium*-infiltrated *N. benthamiana* leaves (**[A]** to **[D]**) or protoplasts (**[E]** to **[H]**) demonstrated dual localization of PPR2263 and MEF29 (At4g30700) in mitochondria and chloroplasts. Fluorescent signals were visualized using confocal laser scanning microscopy.
(A) PPR2263:GFP (green).
(B) Mitochondrial marker protein FDH from potato (FDH:RFP; red).
(C) and **(G)** Chlorophyll autofluorescence (blue).
(D) and **(H)** Merged images.
(E) MEF29:RFP (red).
(F) Mitochondrial marker protein FDH from potato (FDH:GFP; green).

loss of detectable editing at site *nad5*-1550 (Figure 5A). No other editing defects in the same transcript or in other mitochondrial transcripts were detected in this mutant. Since both the *Arabidopsis* and the maize protein showed dual targeting, we also analyzed 34 known editing sites in the *Arabidopsis* chloroplasts but found all of these sites to be edited as in wild-type plants. We accordingly renamed the identified *Arabidopsis* protein MEF29.

Guided by the results in *Arabidopsis*, we focused the investigation of editing defects in maize on the mitochondrial *NADH dehydrogenase* (*nad*) gene family. The only defect detected by direct sequencing of RT-PCR products concerned *nad5*, where editing at *nad5*-1550, the same position as in *Arabidopsis*, was not detectable in *ppr2263* seedlings (Figure 5A). No editing defects were observed in the remaining family members *nad1*,

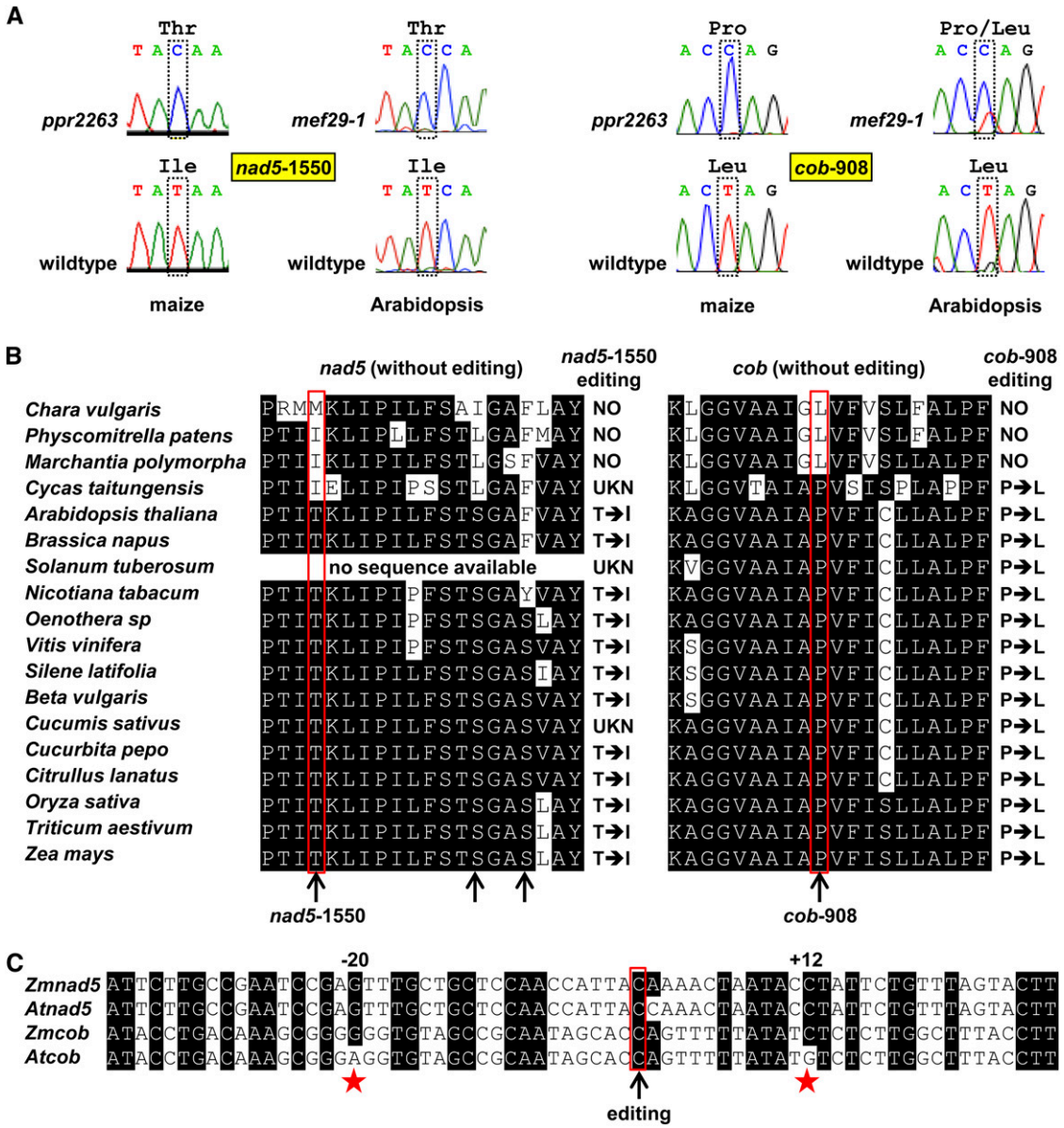

Figure 5. RNA Editing of the *nad5*-1550 and *cob*-908 Sites in Maize *ppr2263* and the *Arabidopsis mef29* Mutants.

(A) Analysis of RNA editing in *nad5* (left) and *cob* transcripts (right). RT-PCR products containing the *nad5*-1550 or *cob*-908 editing sites (dashed frame) were directly sequenced.

(B) Partial alignment of amino acid sequences deduced from genomic DNA of *nad5* or *cob*. The amino acids affected by RNA editing in some of the species are indicated by arrows. Editing information was retrieved from the GenBank/EMBL sequence annotations, from the RNA Editing Database (Picardi et al., 2007), and from dedicated publications (Mower and Palmer, 2006; Alverson et al., 2010; Picardi et al., 2010; Salmans et al., 2010).

(C) Partial alignment of *nad5* and *cob* mitochondrial genomic DNA sequences from maize and *Arabidopsis* around the editing site recognized by PPR2263/MEF29 (arrow). Stars indicate bases conserved between *nad5* and Zm-*cob* but not At-*cob*.

nad2, *nad3*, *nad4*, *nad4L*, *nad6*, *nad7*, and *nad9*. Editing of the *nad5*-1550 site was restored in *ppr2263* mutants after complementation with the *PPR2263* transgene.

Both in maize and in *Arabidopsis*, the *nad5*-1550 editing event led to the presence of an Ile rather than a Thr residue in the deduced amino acid sequence. An alignment of amino acid sequences deduced from genomic DNA of 17 plant species showed that this replacement improved conservation at this residue (Figure 5B). In fact, an Ile residue was encoded in the green alga *Chara vulgaris*; the liverwort *Marchantia polymorpha*, a member of the only plant family not exhibiting RNA editing (Rüdinger et al., 2008); the moss *Physcomitrella patens*, which does not show editing at this site (Rüdinger et al., 2009); and the gymnosperm *Cycas taitungensis*. Angiosperms encoded a Thr residue triplet that was edited to an Ile codon in all species with information available regarding *nad5* editing (Figure 5B).

Normal Complex I Activity, Complex III Deficiency, and Alternative Oxidase Induction in *ppr2263*

To investigate whether the lack of *nad5*-1550 editing affected the activity of complex I, mitochondrial protein complexes isolated from 10-d-old etiolated wild-type or *ppr2263* seedlings were separated on blue native gels and subjected to activity stains for complex I (Figure 6A). No notable difference was observed between the wild type and mutant. However, the band likely corresponding to complex III was unexpectedly missing in the *ppr2263* mutant. To identify unambiguously the missing band, a blot was assayed for the well-documented peroxidase activity of complex III (Figures 6B and 6C). Indeed, peroxidase activity was extremely reduced, indicating a major deficiency of complex III in the *ppr2263* mutant.

A well-characterized defense mechanism against a permanent block of the electron transfer chain is an increase in the alternative respiratory pathway characterized by alternative oxidase (AOX), for example, in maize *nonchromosomal stripe* (*ncs*) mutants (Karpova et al., 2002). Indeed, an immunoblot with a monoclonal anti-AOX antibody (Finnegan et al., 1999) demonstrated among other changes a strong induction of AOX2 in the *ppr2263* mutant (Figures 6D and 6E).

Alteration of *cob*-908 Editing in *ppr2263* and *mef29-1*

Intrigued by the deficiency of complex III, the *cob* gene coding for cytochrome b, the *ccmB*, *ccmC*, *ccmFC* ,and *ccmFN* genes involved in cytochrome c maturation, and the *cox1*, *cox2*, and *cox3* genes coding for cytochrome c oxidase were checked for editing defects in the *ppr2263* maize mutant. The only observed defect was a lack of detectable C-to-U editing at site *cob*-908 (Figure 5A), which was restored in the presence of the *PPR2263* transgene. Sequencing of this site in the *Arabidopsis mef29-1* mutant showed that editing was diminished but clearly detectable, explaining why this site had not been picked up by the SNaPshot assay.

The editing of *cob*-908 changed a Pro residue to a Leu residue in the deduced amino acid sequence of cytochrome b (Figure 5B). As in the case of the *nad5*-1550 site, this change enhanced conservation at this position. Nonvascular plants known to lack *cob*-908 editing encoded a Leu residue, whereas all vascular plants for which we could find editing information showed Pro-to-Leu editing.

An alignment of the putative PPR2263/MEF29-1 target sequences in *nad5* and *cob* revealed an identity of 49%, a value substantially higher than the 25% expected between unrelated sequences (Figure 5C). Interestingly, the conservation between the

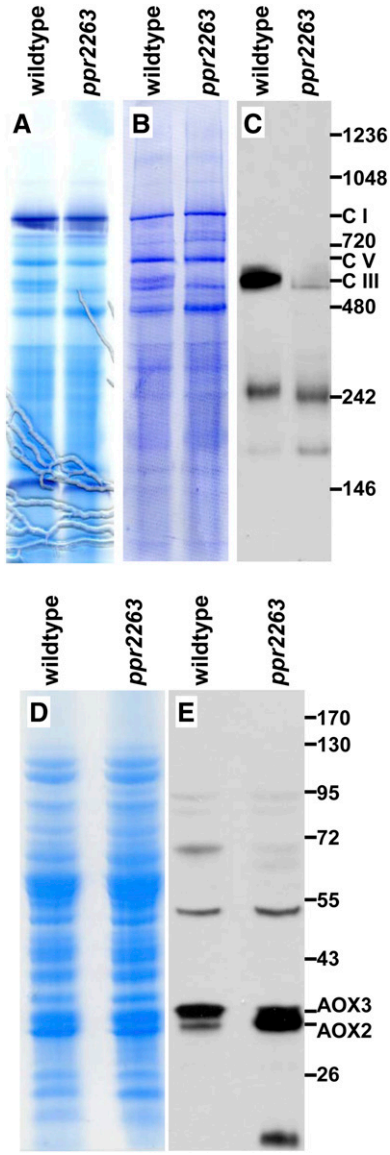

Figure 6. Protein Gels of Mitochondrial Extracts from Etiolated Wild-Type and *ppr2263* Seedlings at 10 DAS.

(A) Blue native (BN) gel after activity stain for complex I and coloration with Coomassie blue.
(B) PVDF membrane after blotting of BN gel and coloration with Coomassie blue.
(C) PVDF membrane after blotting of BN gel and detection of peroxidase activity.
(D) SDS-PAGE after staining with Coomassie blue.
(E) Immunoblot of SDS-PAGE gel with anti-AOX antibody.
[See online article for color version of this figure.]

nad5 and *cob cis*-sequences was higher for *cob* from maize than *cob* from *Arabidopsis* when compared with either *nad5* gene.

Expression of Representative Organelle Genes in *ppr2263*

To investigate whether the *ppr2263* mutation had an effect on organelle gene expression, we compared the transcript levels of selected mitochondrial, plastid, and nuclear genes representing different gene classes between *ppr2263* and wild-type seedlings (see Supplemental Figure 3 online). All mitochondrial genes tested had increased transcript levels in the mutant: *nad3*, *nad4*, and *nad5* encoding different subunits of NADH dehydrogenase (complex I), *cox2* encoding a subunit of cytochrome c oxidase (complex IV), *atp1* and *atp6* encoding subunits of ATP synthase (complex V), and *rpl16* and *rps3* encoding proteins of the large and small ribosomal subunits. In chloroplasts, *psbA* and *petA* transcribed by the plastid-encoded plastid RNA polymerase had decreased expression levels in the *ppr2263* mutant, whereas *rpoB* and *clpP* transcribed by nuclear-encoded plastid RNA polymerase showed a slight increase and no significant change, respectively (see Supplemental Figure 3 online). Investigating the possibility of a retrograde signal on nuclear genes, we detected a twofold upregulation of *TRANSLATIONALLY CONTROLLED TUMOR PROTEIN* but no change in *TARGET OF RAPAMYCIN* expression in the mutant (see Supplemental Figure 3 online). Taken together, these results led to the conclusion that the lesion in *PPR2263* affected transcription in all tested cellular compartments and had a generalized, positive effect on mitochondrial transcript levels as previously observed in respiratory mutants (Meyer et al., 2009; Sung et al., 2010; Kuhn et al., 2011).

Compromised Mitochondrial Ultrastructure in *ppr2263*

To determine if the observed defects in mitochondrial and chloroplast RNA metabolism had repercussions on the morphology of these organelles, we compared their ultrastructure in wild-type and *ppr2263* seedlings at 15 d after sowing (DAS) by transmission electron microscopy (Figure 7). No striking differences in the number of mitochondria per cell or in mitochondrial sizes were observed between the wild type and mutant. However, the majority of the mutant mitochondria had a strongly altered ultrastructure in which the granules were a lot less abundant and the cristae formed by the inner membrane strongly reduced or completely missing (Figures 7A to 7D). Whereas such aberrant mitochondria accounted for <10% in wild-type leaves, they were predominant in mutant leaves where they constituted up to 70% of the population. One may hypothesize that the structurally altered mitochondria were likely nonfunctional or at least less functional than mitochondria with a normal ultrastructure.

A parallel examination of the chloroplast ultrastructure in the same wild-type and mutant leaf cells did not reveal any differences in size, structure, or inner or outer membrane organization, neither in mesophyll nor bundle sheath cells (Figures 7E and 7F). Taken together, the data suggested that the main cellular defect of the *ppr2263* mutant concerned mitochondria and not chloroplasts.

Altered Electron Transport but Normal Gas Exchange in *ppr2263*

Since mitochondria are the center of the cellular respiration, it was tempting to explain the reduced growth of the *ppr2263* mutant by a lack of energy furnished by mitochondria through cellular respiration. To test this hypothesis, we used the 2,3,5-triphenyltetrazolium chloride (TTC) reduction assay (Gibon et al., 2000). TTC has a high redox potential and can be reduced by mitochondrial dehydrogenases to triphenylformazan (TF), reflecting to some extent mitochondrial activity (Zapata et al., 1991). Leaf discs cut from 12-DAS wild-type seedlings produced 2.44-fold more TF than leaf discs of *ppr2263* seedlings of the same age and 2.35-fold more TF than leaf discs of *ppr2263* seedlings of comparable size (28 DAS; Figure 8A).

Subsequent experiments evaluating the gas exchange of 28-DAS *ppr2263* seedlings with wild-type seedlings of the same age (28 DAS) or the same size (12 DAS) did not reveal any significant differences in photosynthesis (Figure 8B; see Supplemental Figure 4 online), day respiration (Figure 8C), or respiration at the end of the night (Figure 8D). These findings suggested that the altered electron

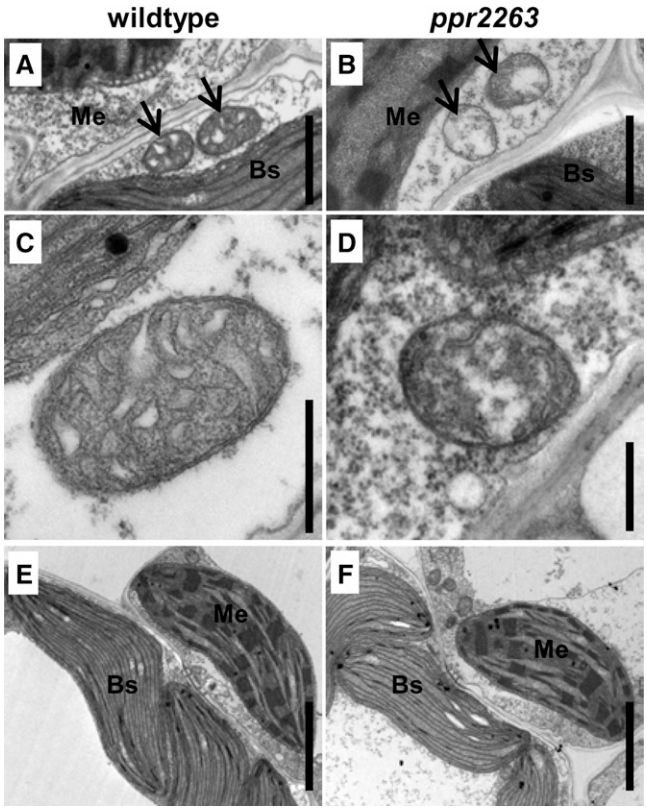

Figure 7. Organelle Ultrastructure in Wild-Type and *ppr2263* Leaves.

Transmission electron micrographs of leaves from wild-type (**[A]**, **[C]**, and **[E]**) and *ppr2263* (**[B]**, **[D]**, and **[F]**) seedlings 16 DAS. Samples were taken at mid-morning.

(A) Normally structured mitochondria (arrows) in a bundle sheath cell (Bs) close to a mesophyll cell (Me).

(B) Mitochondria with altered ultrastructure (arrows) in a mesophyll cell close to a bundle sheath cell.

(C) Magnified view of a mitochondrion with normal ultrastructure.

(D) Magnified view of a mitochondrion with altered ultrastructure.

(E) Bundle sheath and mesophyll chloroplasts in the wild type.

(F) Bundle sheath and mesophyll chloroplasts in *ppr2263*.

Bars = 1 mm in **(A)** and **(B)**, 0.25 mm in **(C)** and **(D)**, and 2 mm **(E)** and **(F)**.

transport did not have a major impact on CO_2 gas exchange, as previously reported for certain respiratory mutants (Meyer et al., 2009).

DISCUSSION

The maize mutant *ppr2263* carries a *Mutator* insertion leading to a truncated protein lacking three of its 13 PPR repeats as well as the C-terminal E/E+ and DYW domains. The reduced growth of vegetative and reproductive organs as well as the changes in mitochondrial ultrastructure, gene expression, and AOX levels are correlated with and possibly caused by a lack of detectable RNA editing at the *cob*-908 site and the resulting loss of mitochondrial complex III (cytochrome c reductase; EC 1.10.2.2), whereas the lack of detectable RNA editing at the *nad5*-1550 site does not seem to affect mitochondrial complex I (NADH:ubiquinone oxidoreductase; EC 1.6.99.3).

Maize Kernel and Plant Growth Retardation in *ppr2263*

Isolated in a screen for *defective kernel* and *miniature* mutants, the *ppr2263* mutant fulfills only part of the definition of *miniature* mutants (Lowe and Nelson, 1946). While the mutant presents the kernel phenotype with smaller but morphogenetically normal kernels capable of germination, it does not fit the vegetative phenotype, since *ppr2263* mutants grow slower than wild-type siblings, exhibit reduced plant height, and hardly reach sexual maturity, in contrast with typical *miniature* mutants, such as *miniature1* (*mn1*) (Cheng et al., 1996) or *reduced grain filling1* (Maitz et al., 2000). Consequently, one may expect that the mutation affects a general cellular function rather than a kernel-specific function such as the cell wall invertase IncW2 in the *mn1* mutant (Cheng et al., 1996). Although the *ppr2263* mutant shares the reduced plant height of the maize *dwarf1* to *dwarf8* mutants (Olson, 1954; Phinney, 1956), it does not possess the other attributes of these *dwarf* mutants that are all affected in the biosynthesis of gibberellic acid. The absence of broad, erect, dark-green leaves, reduced internode length, and fully developed anthers in the ear suggests that *ppr2263* is not affected in gibberellic acid metabolism.

In the vegetative apparatus of the *ppr2263* mutant, the leaves formed are not only smaller and less numerous than in wild-type siblings, they also take longer to appear. With regard to seed development, embryo and endosperm are not only smaller at maturity, they also take longer to reach a given developmental stage. Such generalized growth defects independent of organ or age are reminiscent of mitochondrial mutants. This view is reinforced by physiological defects, such as the deficiency in mitochondrial complex III and the reduction in electron transport to ~40% of the wild-type rate, as well as cellular defects, such as the loss of inner mitochondrial membrane organization.

Evolutionary Conservation of *nad5*-1550 and *cob*-908 Editing Activity between PPR2263 and MEF29

On the molecular level, maize *ppr2263* and *Arabidopsis mef29-1* share the lack of detectable editing at the *nad5*-1550 site, whereas *cob*-908 editing is not detected in *ppr2263* and strongly reduced in *mef29-1*. The target site conservation between maize and *Arabidopsis* as well as the next-neighbor position in phylogenetic trees show MEF29 and the PPR2263 to be true functional orthologs. Thus, we identified an orthologous RNA editing factor pair sharing their target sites between a monocot and a dicot plant. The high similarity observed between the two PPR proteins suggests them to be derived from a common ancestor and to have been conserved by functional constraints. This selective pressure may be due to the need for RNA editing at *nad5*-1550 and/or *cob*-908.

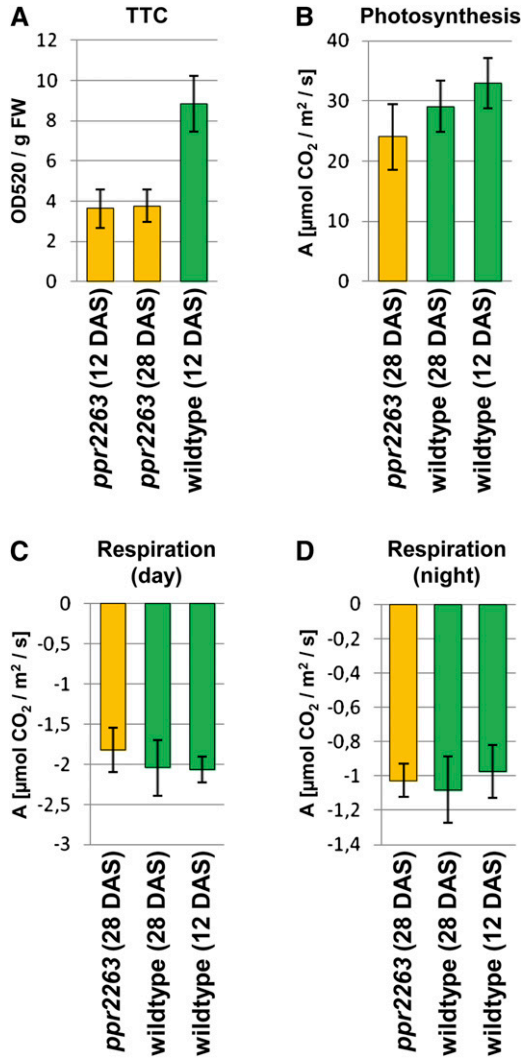

Figure 8. Electron Transport, Photosynthesis, and Respiration in Wild-Type and *ppr2263* Leaves.

(A) Mitochondrial electron transport measured by TTC assay. FW, fresh weight.
(B) Net photosynthetic rate measured with infrared gas analyzer at a PAR of 1500 µmol photons m^{-2} s^{-1}.
(C) Day respiration measured as the y-intercept of the photosynthesis versus PAR curve.
(D) Night respiration measured at the end of the night.
Error bars represent the SD with n = 3 in **(A)** and n = 5 in **(B)** to **(D)**. Photosynthesis versus PAR response curves can be found in Supplemental Figure 4 online.
[See online article for color version of this figure.]

Editing at *nad5*-1550 causes a Thr-to-Ile change in the conserved C-terminal domain (pfam06455) of NAD5, whereas editing at *cob*-908 is responsible for a Pro-to-Leu change in the conserved C-terminal domain (pfam00032) of cytochrome b. In both cases, the residue obtained by editing (Ile or Leu) seems to be ancestral because it is present in nonvascular plants, and in particular in *M. polymorpha* not exhibiting any RNA editing (Rüdinger et al., 2008), and in *P. patens* not showing editing at these sites (Rüdinger et al., 2009). All vascular plants for which editing information is available encode the same nonedited residue (Thr or Pro) and convert it to the edited residue (Ile or Leu). The evolutionary conservation of an Ile residue in NAD5 and a Leu residue in cytochrome b points to functional constraints and suggests that *nad5*-1550 and *cob*-908 editing is important for NAD5 and cytochrome b function, respectively.

The nucleotide sequences around the *nad5*-1550 and *cob*-908 editing sites show elevated similarity as expected for conserved target sites of bona fide RNA binding proteins, such as PPR2263/MEF29. Interestingly, conservation is higher between *nad5* and *cob* from maize than between *nad5* and *cob* from *Arabidopsis*. This finding may indicate that in *Arabidopsis* MEF29 is in the process of losing its capacity to edit the *cob*-908 site and that this function is taken over by another PPR protein, explaining the fact that *cob*-908 editing is only partially lost in the *mef29-1* mutant. Alternatively, *mef29-1* may not be a complete knockout line, since the T-DNA insertion is located in the C-terminal DYW domain. The truncated protein may be sufficient to edit the *cob*-908 site partially but not the *nad5*-1550 site.

Absence of *nad5* and *cob* Editing and Reduced Growth in *ppr2263*

The *ppr2263* mutation is the first reported maize mutation responsible for an editing defect; consequently, there is no precedent of associated phenotypes in maize. The only other monocot editing mutant is the rice *opaque and growth retardation1* mutant, which is affected in the correct editing of the mitochondrial *nad2* gene and is characterized by delayed seed germination, retarded growth, dwarfism, and sterility (Kim et al., 2009). Similarly, the *Arabidopsis slow growth1* mutant with altered editing of *nad4* and *nad9* displays late germination, slow growth, and delayed development phenotypes and produces shrunken seed (Sung et al., 2010). Finally, in *P. patens*, the disruption of *PPR79* led to no detectable editing at the *nad5*-598 site and resulted in severe growth retardation of protonemata colonies (Uchida et al., 2011).

By contrast, the majority of the mitochondrial editing mutants in *Arabidopsis* do not show any notable growth defects, and the mutants *mef1* (Zehrmann et al., 2009), *mef9* (Takenaka, 2010), *mef11*/*loi1* (Verbitskiy et al., 2010; Tang et al., 2010), *mef14* (Verbitskiy et al., 2011), *reme1* (Bentolila et al., 2010), and *mef18* to *mef22* (Takenaka et al., 2010) display no gross disturbance in their growth or development patterns. This is also the case of the *Arabidopsis mef29-1* mutant sharing disturbed *nad5*-1550 and *cob*-908 editing with *ppr2263*. Whereas development is slightly delayed (e.g., bolting and flower set start ~1 to 2 d later than in wild-type plants), the analysis of the global mitochondrial activity by the TTC analysis did not reveal any clear difference between mutant and the wild type.

Several alternative scenarios can explain the different growth behaviors of *Arabidopsis mef29-1* and maize *ppr2263*, the most plausible ones attributing the severe growth phenotype of the maize *ppr2263* mutant to the lack of detectable *nad5*-1550 and/or *cob*-908 editing. Formally it cannot be excluded that the severe growth phenotype in maize is caused by additional functions of PPR2263 and in particular editing of additional sites. However, the simplest hypothesis compatible with all data suggests that loss of *nad5*-1550 editing has no or very little effect on plant growth both in maize *ppr2263* and *Arabidopsis mef29-1*, whereas loss of *cob*-908 editing causes a severe deficiency in mitochondrial complex III, which in turn is responsible for reduced growth in maize *ppr2263.* In *Arabidopsis mef29-1*, the residual *cob*-908 editing is sufficient to assure normal growth.

It is not trivial to exclude a contribution of the *nad5*-1550 editing defect to the *ppr2263* phenotype since slow growth has been reported for numerous complex I mutants, for example, in *Nicotiana sylvestris* (Gutierres et al., 1997), rice (Kim et al., 2009), and *Arabidopsis* (Meyer et al., 2009; Sung et al., 2010; Yuan and Liu, 2012). The maize mutant with the most similar plant phenotype to *ppr2263* is a homoplasmic *ncs2* mutant, which carries exclusively mutant mitochondria with a small deletion in the *nad4* gene encoding a subunit of NADH dehydrogenase (Yamato and Newton, 1999). Electron transport in the *nad4*-deficient mutant seems to occur via a partially assembled complex I (Karpova and Newton, 1999) as well as by an increase of the alternative respiratory pathway via *aox2* (Karpova et al., 2002), whereas there is no evidence for a compensatory increase of exogenous NADH dehydrogenases. The *ppr2263* mutant shares with the homoplasmic *ncs2* mutant nearly all reported phenotypic traits, which consist of very narrow and short leaves, an ~2.5-fold decrease in plant height, an approximately twofold decrease of leaf number, and the development of a small tassel with underdeveloped anthers. The only exception is the formation of a small ear on the *ppr2263* mutant, whereas there is no indication of ear formation in the homoplasmic *ncs2* mutant (Yamato and Newton, 1999). However, the normal activity of complex I in maize *ppr2263* and the absence of strong growth defects in *Arabidopsis mef29-1* fully sharing the *nad5*-1550 editing defect argue against an effect of this editing defect in complex I on plant growth.

On the other hand, the near absence of complex III was the only detected difference in mitochondrial complexes and the lack of detectable *cob*-908 editing the only observed editing defect concerning complex III or IV. Strongly reduced electron transport through complex III has been reported to cause a semidwarf growth habit in the *Arabidopsis ppr40-1* mutant (Zsigmond et al., 2008). In addition, in *ppr40-1*, AOX was induced just like in *ppr2263*. All these observations can be synthesized in a model in which lack of *cob*-908 editing causes the absence of complex III and altered electron transport from complex I and complex II directly to AOX as terminal electron acceptor. Oxidation of NADH by complex I and $FADH_2$ by complex II are intact, and O_2 is consumed by AOX. Due to the lack of electron transport through complex III and IV, two-thirds of the proton translocation is lost and the proton gradient driving complex V (ATP synthase) strongly diminished leading to reduced ATP production, explaining the general growth deficit observed in *ppr2263*. For future research, the *ppr2263* mutant provides a powerful tool to investigate the biochemical and physiological consequences of complex III

deficiency in isolated mitochondria and at the whole-plant level, both under normal and stress conditions.

METHODS

Plant Material and Culture

The maize (*Zea mays*) inbred lines A188 and F252 (gifts of Alain Charcosset, Le Moulon, France), the *ppr2263* mutant (*Mutator*-induced Biogemma mutant collection; this study), and the transgenic plants overexpressing *PPR2263* were grown in an S2 greenhouse with a 16-h illumination period (100 Wm^{-2}) at 24/19°C (day/night) and without control of the relative humidity as described (Javelle et al., 2010). The culture conditions for mutant *mef29-1* (SALK_096438 BN) and wild-type (ecotype Columbia) *Arabidopsis thaliana* plants have also been described (Takenaka and Brennicke, 2007).

Light Microscopy of Cytological Sections

Immature wild-type and mutant kernels were harvested from the ear of a self-pollinated heterozygous plant at 9 and 24 DAP and cut along the longitudinal axis in three equal parts. The central slice containing the embryo was fixed for 1 h at room temperature in 100 mM Dulbecco's phosphate buffer (Lonza Walkersville) with 1% paraformaldehyde and 3% glutaraldehyde. The fixed material was dehydrated in a graded ethanol series (10, 30, 50, 70, 90, and 100% ethanol), embedded in Technovit 7100 resin (Kulzer Heraeus) according to the manufacturer's instructions, sectioned at 6 to 8 μm with a HM3555 microtome (Microm Microtech), and stained with Schiff reagent (Sigma-Aldrich). The sections were observed with an Axio Imager M2 microscope (Zeiss) coupled with an Axio Cam MRC digital camera (Zeiss).

Transmission Electron Microscopy

Wild-type and mutant leaf squares or embryos were fixed overnight at room temperature in 0.2 M cacodylate buffer, pH 7.1, with 2% glutaraldehyde. The fixed tissue was then washed in cacodylate buffer and treated for 1 h with 1% osmium tetroxide, followed by dehydration in a graded ethanol series (see above) and embedding in agar low viscosity resin (Agar Scientific). Ultrathin sections of 80 nm were cut using a diamond knife and lifted onto 2-mm copper grids. Grids were stained in 2% uranylacetate and lead citrate prior to observation with a JEOL 1200EX transmission electron microscope.

cDNA Display of Genes with *Mutator* Insertions (MuExpress)

Mutant and wild-type kernels were harvested from the *ppr2263* mutants at 13 DAP, the first stage when mutant kernels of all 300 mutants of the collection can be distinguished unambiguously from wild-type kernels. RNA was isolated from two mutant pools and one wild-type pool, each pool consisting of three kernels, following previously described methods (Javelle et al., 2010). The RNA was subjected to 5′ and 3′ RACE reactions using the SMART RACE cDNA amplification kit (Clontech), with nested primers in the highly conserved inverted repeats of *Mutator* in combination with nested primers in the adapters ligated to either the 5′ or 3′ end (see Supplemental Figure 1A online). The RACE products were separated on LI-COR gels according to the recommendations of the supplier (LI-COR Biosciences) to detect bands present only in the two mutant samples and absent in the wild-type sample (see Supplemental Figure 1B online). Candidate bands were isolated from high-resolution agarose gels, cloned, and sequenced. Based on the flanking sequence, additional primers were designed and used in combination with a primer in the terminal inverted repeat of *Mutator* to confirm the differential expression in the cDNA samples that had served for the RACE reaction. All primers used are listed in Supplemental Table 1 online.

Subcellular Localization of PPR2263

To generate a translational PPR2263:GFP fusion, the full-length open reading frame of *PPR2263* lacking its stop codon was amplified by PCR with primers PPR-E2263-attB1 and PPR2263w/oSTPattB2 (see Supplemental Table 1 online) on genomic DNA from maize inbred line B73 and recombined via the entry vector pDONR-Zeo into the binary vector pK7FWg2 (Karimi et al., 2002) by GATEWAY site-specific recombination (Invitrogen). The binary construct, in which the *PPR2263*:*GFP* chimera was under the control of the cauliflower mosaic virus *35S* promoter, was transferred into *Agrobacterium tumefaciens* strain C58pMP90. Using established protocols (van Herpen et al., 2010), the resulting strain was coinfiltrated into *Nicotiana benthamiana* leaves with a strain harboring the 35S:P19 plasmid expressing the silencing suppressor p19 of tomato bushy stunt virus (Voinnet et al., 2003) and a third strain containing the mitochondrial marker construct FDH:RFP2 (courtesy of Catherine Colas des Francs-Small). In the latter construct, formate dehydrogenase from potato (*Solanum tuberosum*; Ambard-Bretteville et al., 2003) had been amplified with primers ATG1 and FHD-R (see Supplemental Table 1 online) and cloned into pGreen (Vain et al., 2003). GFP, RFP, and chloroplast autofluorescence were detected 3 d after infiltration on an LSM 710 inverted confocal spectral microscope (Zeiss), with two sequential excitations for every acquisition: the first at 488 nm with an emission collected from 501 to 548 nm for the GFP signal, and the second at 561 nm with two collected emissions from 569 to 608 nm for the RFP signal and from 638 nm to 742 nm for autofluorescence.

The full-length open reading frame or the 300 bp encoding the first 100 amino acids of *MEF29* were amplified (see Supplemental Table 1 online) and recombined via the entry vector pDNR207 to the pGreen 0229 destination vector containing the *GFP* or *RFP* gene under the 35S promoter (Lurin et al., 2004). Transformed C58C1 *Agrobacterium* strains were used for infiltration of *N. benthamiana* protoplasts, which were observed under a confocal microscope (Leica TCS-NT) allowing the detection of GFP (excitation/emission: 479 nm/509 nm; filter BP530/30) and RFP (DsRed2: excitation/emission: 558 nm/583 nm; filter BP580/80).

RNA Extraction and Reverse Transcription

Approximately 250 mg of fresh tissue was quick frozen in liquid nitrogen and ground to powder with a mortar and pestle. Total RNA was extracted with 1 mL TRI reagent according to the instructions of the supplier (Molecular Research Center). After ethanol precipitation, the RNA was resuspended in 30 μL RNase-free water and treated with RNase-free DNase. The DNase was inactivated according to the instructions of the supplier (Ambion). Approximately 5 μg of total RNA were reverse transcribed using random hexamers (Amersham Biosciences) and reverse transcriptase without RNaseH activity (Fermentas) in a final volume of 20 μL. For RT-PCR experiments, 2 μL of a 50-fold dilution of the cDNA in water were used in a volume of 20 μL.

SNaPshot Assays and Mutant Analysis

Arabidopsis DNA or RNA was prepared from leaves as described (Takenaka and Brennicke, 2007). The status of RNA editing at specific sites was screened by multiplexed single-base extension (Takenaka and Brennicke, 2009). Sequence analyses were obtained commercially from 4base lab (Reutlingen, Germany) or from Macrogen (Seoul, Korea).

qRT-PCR

The cDNA was diluted 50 times and 2 μL used in a volume of 20 μL containing 10 μL Platinum SYBR Green qPCR SuperMix UDG according to the instructions of the supplier (Invitrogen) to carry out quantitative PCR on an Applied Stepone Plus (Applied Biosystem). Dilutions series (2n with $n = 0$ to 7) of a mixture of all cDNA within a comparison were used to fix the

CT (threshold cycle). Each reaction was made in a duplicate, and the gene expression levels relative to the nuclear *18S* rRNA reference gene were calculated by the ΔΔcycle threshold method (Schmittgen and Livak, 2008). All the primers used are listed in Supplemental Table 1 online.

Plant Transformation for *ppr2263* Complementation

The plasmid used for the production of *PPR2263-OE* plants contained the backbone of vector pSB11 (Ishida et al., 1996), a Basta resistance cassette (rice [*Oryza sativa*] *Actin* promoter and intron, *Bar*, and *Nos* terminator) next to the right border, and the *PPR2263* coding sequence (primers PPR-E2263-attB1and PPR-E2263-attB2, including a 6-HIS tag before the STOP codon; see Supplemental Table 1 online) under the control of the rice *Actin* promoter next to the left border. *Agrobacterium*-mediated transformation of maize inbred line A188 was executed according to a published protocol (Ishida et al., 2007). For each transformation event, the number of T-DNA insertions was evaluated by qRT-PCR, and the integrity of the transgene was verified by PCR with primers situated in the *AtSac66* terminator downstream of *PPR2263* next to the left border.

Blue Native Gels and Activity Stains

Mitochondria were isolated from 10-DAS etiolated seedlings on Percoll gradients (Wittig et al., 2006). After separation of mitochondrial protein complexes with the NativePAGE Bis-Tris Gel system (Invitrogen), the gels were either stained for complex I activity prior to staining with Coomassie Brilliant Blue (Wittig et al., 2006) or transferred to polyvinylidene fluoride (PVDF) membranes (Millipore). Peroxidase activity was visualized with the Amersham ECL Western Blotting Detection Reagents (GE Healthcare) prior to staining of the membrane with Coomassie Brilliant Blue. For immunoblotting, mitochondrial proteins were separated by SDS-PAGE, transferred to nitrocellulose membranes, incubated with a monoclonal anti-AOX antibody (Finnegan et al., 1999) provided by Etienne Meyer (CNRS, Strasbourg), and revealed by electrochemical luminescence by use of the iBlot Western Detection Kit (Invitrogen).

TTC Reduction Assay

The TTC assay was based on the protocol of Steponkus (Steponkus and Lanphear, 1967) with the modifications of Gibon et al. (2000). The TTC reduction was expressed as absorbance at 520 nm per g fresh weight.

Gas Exchange Measurements

Gas exchange measurements were performed in the greenhouse on the youngest ligulated leaf (generally leaf #7 of 28-DAS wild-type or *ppr2263* plants or leaf #5 of 12-DAS wild-type plants) with a 2 × 3-cm leaf chamber of a Li-6400 infrared gas analyzer (LiCor) with a red-blue light-emitting diode light source. Prior to the measurements, leaves were equilibrated for 30 min at an ambient CO_2 of 400 μmol mol^{-1}, a PAR of 1500 μmol photons m^{-2} s^{-1}, and a leaf temperature of 28°C. Measurements were taken at decreasing PAR (typically 1500, 1000, 800, 100, 75, 60, 45, 30, 15, and 0 μmol photons m^{-2} s^{-1}) allowing equilibration at each step. Day respiration was estimated as the y-intercept of the photosynthesis/irradiance curve, whereas night respiration was estimated from the gas exchange rate during the last 2 h of the night.

Accession Numbers

Sequence data corresponding to the genes described in this article can be found in the Arabidopsis Genome Initiative or Maize Sequence databases under the following accession numbers: *MEF29*, At4g30700; *PPR2263*, AC215198.3_FG002. The GenBank/EMBL accession numbers for mitochondrial genomic *nad5* and *cob* sequences are as follows: *Chara vulgaris*, AY267353.1; *Physcomitrella patens*, AB251495.1; *Marchantia polymorpha*, M68929.1; *Cycas taitungensis*, AP009381.1; *Arabidopsis*, JF729202.1; *Brassica napus*, FR715249.1; *Nicotiana tabacum*, BA000042.1; *Vitis vinifera*, GQ220325.1; *Silene latifolia*, HM562727.1; *Beta vulgaris*, BA000024.1; *Cucumis sativus*, HQ860792.1; *Cucurbita pepo*, GQ856148.1; *Citrullus lanatus*, GQ856147.1; *O. sativa*, DQ167400.1; *Triticum aestivum*, GU985444.1; *Z. mays*, DQ490952.1.

Supplemental Data

The following materials are available in the online version of this article.

Supplemental Figure 1. *Mutator* cDNA Display (MuExpress Technique).

Supplemental Figure 2. Alignment of PPR2263 with Its Putative Orthologs in Rice and *Arabidopsis*.

Supplemental Figure 3. Expression of Mitochondrial, Plastid, and Nuclear Genes in the *ppr2263* Mutant.

Supplemental Figure 4. Photosynthesis and Respiration in Wild-Type and *ppr2263* Leaves.

Supplemental Table 1. Primers Used for the Study.

ACKNOWLEDGMENTS

We thank Christelle Boule for help with electron microscopy, Eve-Isabelle Pecheur for help with the TTC assay, Etienne Meyer for the anti-AOX antibody, Gregorio Hueros for LiCOR analysis, Barbara Härtel for evaluation of chloroplast editing, Catherine Colas des Francs-Small for the mitochondrial marker construct, and Claire Lurin for the mitochondria reporter vector used for the subcellular localization. We also thank Gabriella Consonni, Martine Devic, Nathalie Depège-Fargeix, Gwyneth Ingram, Yves Gibon, Claire Lurin, Bertrand Muller, Etienne Meyer, and Axel Brennicke for constructive discussions and critical reading of the manuscript. We thank Isabelle Desbouchages, Alexis Lacroix, and Priscilla Angelot for maize culture, and Hervé Leyral and Claudia Bardoux for excellent technical assistance. We also acknowledge the contribution of the PLATIM (Christophe Chamot) and AG (Bariza Blanquier) platforms of the Structure Fédérative de Recherche Biosciences Gerland-Lyon Sud (UMS344/US8). The work was financed in part by the Génoplante project "MuExpress" (ANR-06-ERAPG-001), which also provided for S.M. D.S. was supported by a PhD fellowship of the French Ministry of Higher Education.

AUTHOR CONTRIBUTIONS

D.S., M.T., and P.M.R. designed the research. D.S., S.M., V.V., G.G., A.D., P.C., M.D., L.H., V.G., and M.T. performed research. D.S., S.M., V.V., M.D., V.G., M.T., and P.M.R. analyzed data. D.S. and P.M.R. wrote the article.

Received August 31, 2011; revised January 12, 2012; accepted January 18, 2012; published February 7, 2012.

REFERENCES

Alverson, A.J., Wei, X., Rice, D.W., Stern, D.B., Barry, K., and Palmer, J.D. (2010). Insights into the evolution of mitochondrial genome size from complete sequences of *Citrullus lanatus* and *Cucurbita pepo* (Cucurbitaceae). Mol. Biol. Evol. **27:** 1436–1448.

Ambard-Bretteville, F., Small, I., Grandjean, O., and Colas des Francs-Small, C. (2003). Discrete mutations in the presequence of potato formate dehydrogenase inhibit the in vivo targeting of GFP fusions into mitochondria. Biochem. Biophys. Res. Commun. **311:** 966–971.

Beick, S., Schmitz-Linneweber, C., Williams-Carrier, R., Jensen, B., and Barkan, A. (2008). The pentatricopeptide repeat protein PPR5 stabilizes a specific tRNA precursor in maize chloroplasts. Mol. Cell. Biol. **28:** 5337–5347.

Benne, R., Van den Burg, J., Brakenhoff, J.P., Sloof, P., Van Boom, J.H., and Tromp, M.C. (1986). Major transcript of the frameshifted coxII gene from trypanosome mitochondria contains four nucleotides that are not encoded in the DNA. Cell **46:** 819–826.

Bentolila, S., Elliott, L.E., and Hanson, M.R. (2008). Genetic architecture of mitochondrial editing in *Arabidopsis thaliana*. Genetics **178:** 1693–1708.

Bentolila, S., Knight, W., and Hanson, M. (2010). Natural variation in Arabidopsis leads to the identification of REME1, a pentatricopeptide repeat-DYW protein controlling the editing of mitochondrial transcripts. Plant Physiol. **154:** 1966–1982.

Chateigner-Boutin, A.L., des Francs-Small, C.C., Delannoy, E., Kahlau, S., Tanz, S.K., de Longevialle, A.F., Fujii, S., and Small, I. (2011). OTP70 is a pentatricopeptide repeat protein of the E subgroup involved in splicing of the plastid transcript rpoC1. Plant J. **65:** 532–542.

Chateigner-Boutin, A.L., and Small, I. (2007). A rapid high-throughput method for the detection and quantification of RNA editing based on high-resolution melting of amplicons. Nucleic Acids Res. **35:** e114.

Chateigner-Boutin, A.L., and Small, I. (2010). Plant RNA editing. RNA Biol. **7:** 213–219.

Cheng, W.H., Taliercio, E.W., and Chourey, P.S. (1996). The Miniature1 seed locus of maize encodes a cell wall invertase required for normal development of endosperm and maternal cells in the pedicel. Plant Cell **8:** 971–983.

Cossegal, M., Chambrier, P., Mbelo, S., Balzergue, S., Martin-Magniette, M.L., Moing, A., Deborde, C., Guyon, V., Perez, P., and Rogowsky, P. (2008). Transcriptional and metabolic adjustments in ADP-glucose pyrophosphorylase-deficient bt2 maize kernels. Plant Physiol. **146:** 1553–1570.

Covello, P.S., and Gray, M.W. (1989). RNA editing in plant mitochondria. Nature **341:** 662–666.

D'Andrea, L.D., and Regan, L. (2003). TPR proteins: the versatile helix. Trends Biochem. Sci. **28:** 655–662.

Das, A.K., Cohen, P.W., and Barford, D. (1998). The structure of the tetratricopeptide repeats of protein phosphatase 5: Implications for TPR-mediated protein-protein interactions. EMBO J. **17:** 1192–1199.

Delannoy, E., Stanley, W.A., Bond, C.S., and Small, I.D. (2007). Pentatricopeptide repeat (PPR) proteins as sequence-specificity factors in post-transcriptional processes in organelles. Biochem. Soc. Trans. **35:** 1643–1647.

Ding, Y.H., Liu, N.Y., Tang, Z.S., Liu, J., and Yang, W.C. (2006). Arabidopsis GLUTAMINE-RICH PROTEIN23 is essential for early embryogenesis and encodes a novel nuclear PPR motif protein that interacts with RNA polymerase II subunit III. Plant Cell **18:** 815–830.

Emanuelsson, O., Brunak, S., von Heijne, G., and Nielsen, H. (2007). Locating proteins in the cell using TargetP, SignalP and related tools. Nat. Protoc. **2:** 953–971.

Emanuelsson, O., Nielsen, H., Brunak, S., and von Heijne, G. (2000). Predicting subcellular localization of proteins based on their N-terminal amino acid sequence. J. Mol. Biol. **300:** 1005–1016.

Finnegan, P.M., Wooding, A.R., and Day, D.A. (1999). An alternative oxidase monoclonal antibody recognises a highly conserved sequence among alternative oxidase subunits. FEBS Lett. **447:** 21–24.

Frey, M., Stettner, C., and Gierl, A. (1998). A general method for gene isolation in tagging approaches: amplification of insertion mutagenised sites (AIMS). Plant J. **13:** 717–721.

Fujii, S., and Small, I. (2011). The evolution of RNA editing and pentatricopeptide repeat genes. New Phytol. **191:** 37–47.

Gibon, Y., Sulpice, R., and Larher, F. (2000). Proline accumulation in canola leaf discs subjected to osmotic stress is related to the loss of chlorophylls and to the decrease of mitochondrial activity. Physiol. Plant. **110:** 469–476.

Giegé, P., and Brennicke, A. (1999). RNA editing in Arabidopsis mitochondria effects 441 C to U changes in ORFs. Proc. Natl. Acad. Sci. USA **96:** 15324–15329.

Gutierres, S., Sabar, M., Lelandais, C., Chetrit, P., Diolez, P., Degand, H., Boutry, M., Vedel, F., de Kouchkovsky, Y., and De Paepe, R. (1997). Lack of mitochondrial and nuclear-encoded subunits of complex I and alteration of the respiratory chain in *Nicotiana sylvestris* mitochondrial deletion mutants. Proc. Natl. Acad. Sci. USA **94:** 3436–3441.

Gutiérrez-Marcos, J.F., Dal Prà, M., Giulini, A., Costa, L.M., Gavazzi, G., Cordelier, S., Sellam, O., Tatout, C., Paul, W., Perez, P., Dickinson, H. G., and Consonni, G. (2007). *empty pericarp4* encodes a mitochondrion-targeted pentatricopeptide repeat protein necessary for seed development and plant growth in maize. Plant Cell **19:** 196–210.

Hammani, K., Gobert, A., Hleibieh, K., Choulier, L., Small, I., and Giegé, P. (2011). An *Arabidopsis* dual-localized pentatricopeptide repeat protein interacts with nuclear proteins involved in gene expression regulation. Plant Cell **23:** 730–740.

Handa, H. (2003). The complete nucleotide sequence and RNA editing content of the mitochondrial genome of rapeseed (*Brassica napus* L.): Comparative analysis of the mitochondrial genomes of rapeseed and *Arabidopsis thaliana*. Nucleic Acids Res. **31:** 5907–5916.

Hashimoto, M., Endo, T., Peltier, G., Tasaka, M., and Shikanai, T. (2003). A nucleus-encoded factor, CRR2, is essential for the expression of chloroplast ndhB in Arabidopsis. Plant J. **36:** 541–549.

Ishida, Y., Hiei, Y., and Komari, T. (2007). Agrobacterium-mediated transformation of maize. Nat. Protoc. **2:** 1614–1621.

Ishida, Y., Saito, H., Ohta, S., Hiei, Y., Komari, T., and Kumashiro, T. (1996). High efficiency transformation of maize (*Zea mays* L.) mediated by *Agrobacterium tumefaciens*. Nat. Biotechnol. **14:** 745–750.

Javelle, M., Vernoud, V., Depège-Fargeix, N., Arnould, C., Oursel, D., Domergue, F., Sarda, X., and Rogowsky, P.M. (2010). Overexpression of the epidermis-specific homeodomain-leucine zipper IV transcription factor Outer Cell Layer1 in maize identifies target genes involved in lipid metabolism and cuticle biosynthesis. Plant Physiol. **154:** 273–286.

Karimi, M., Inzé, D., and Depicker, A. (2002). GATEWAY vectors for Agrobacterium-mediated plant transformation. Trends Plant Sci. **7:** 193–195.

Karpova, O.V., Kuzmin, E.V., Elthon, T.E., and Newton, K.J. (2002). Differential expression of alternative oxidase genes in maize mitochondrial mutants. Plant Cell **14:** 3271–3284.

Karpova, O.V., and Newton, K.J. (1999). A partially assembled complex I in NAD4-deficient mitochondria of maize. Plant J. **17:** 511–521.

Kim, S.R., Yang, J.I., Moon, S., Ryu, C.H., An, K., Kim, K.M., Yim, J., and An, G. (2009). Rice OGR1 encodes a pentatricopeptide repeat-DYW protein and is essential for RNA editing in mitochondria. Plant J. **59:** 738–749.

Kuhn, K., Carrie, C., Giraud, E., Wang, Y., Meyer, E.H., Narsai, R., des Francs-Small, C.C., Zhang, B., Murcha, M.W., and Whelan, J. (2011). The RCC1 family protein RUG3 is required for splicing of nad2 and complex I biogenesis in mitochondria of *Arabidopsis thaliana*. Plant J. **67:** 1067–1080.

Liu, S., Dietrich, C.R., and Schnable, P.S. (2009). DLA-based strategies for cloning insertion mutants: Cloning the gl4 locus of maize using Mu transposon tagged alleles. Genetics **183:** 1215–1225.

Lowe, J., and Nelson, O.E. (1946). Miniature seed-A study in the development of a defective caryopsis in maize. Genetics **31:** 525–533.

Lurin, C., et al. (2004). Genome-wide analysis of *Arabidopsis* pentatricopeptide repeat proteins reveals their essential role in organelle biogenesis. Plant Cell **16:** 2089–2103.

Maitz, M., Santandrea, G., Zhang, Z., Lal, S., Hannah, L.C., Salamini,

F., and Thompson, R.D. (2000). rgf1, a mutation reducing grain filling in maize through effects on basal endosperm and pedicel development. Plant J. **23:** 29–42.

Martin, A., et al. (2006). Two cytosolic glutamine synthetase isoforms of maize are specifically involved in the control of grain production. Plant Cell **18:** 3252–3274.

McCarty, D.R., et al. (2005). Steady-state transposon mutagenesis in inbred maize. Plant J. **44:** 52–61.

McElroy, D., Zhang, W., Cao, J., and Wu, R. (1990). Isolation of an efficient actin promoter for use in rice transformation. Plant Cell **2:** 163–171.

Messing, J., and Dooner, H.K. (2006). Organization and variability of the maize genome. Curr. Opin. Plant Biol. **9:** 157–163.

Meyer, E.H., Tomaz, T., Carroll, A.J., Estavillo, G., Delannoy, E., Tanz, S.K., Small, I.D., Pogson, B.J., and Millar, A.H. (2009). Remodeled respiration in ndufs4 with low phosphorylation efficiency suppresses Arabidopsis germination and growth and alters control of metabolism at night. Plant Physiol. **151:** 603–619.

Mower, J.P., and Palmer, J.D. (2006). Patterns of partial RNA editing in mitochondrial genes of *Beta vulgaris*. Mol. Genet. Genomics **276:** 285–293.

Okuda, K., Nakamura, T., Sugita, M., Shimizu, T., and Shikanai, T. (2006). A pentatricopeptide repeat protein is a site recognition factor in chloroplast RNA editing. J. Biol. Chem. **281:** 37661–37667.

Okuda, K., Chateigner-Boutin, A.L., Nakamura, T., Delannoy, E., Sugita, M., Myouga, F., Motohashi, R., Shinozaki, K., Small, I., and Shikanai, T. (2009). Pentatricopeptide repeat proteins with the DYW motif have distinct molecular functions in RNA editing and RNA cleavage in *Arabidopsis* chloroplasts. Plant Cell **21:** 146–156.

Okuda, K., Hammani, K., Tanz, S.K., Peng, L., Fukao, Y., Myouga, F., Motohashi, R., Shinozaki, K., Small, I., and Shikanai, T. (2010). The pentatricopeptide repeat protein OTP82 is required for RNA editing of plastid ndhB and ndhG transcripts. Plant J. **61:** 339–349.

Olson, J.W. (1954). A comparison of leaf number, internode and mesocotyl lengths in dwarf1 and normal *Zea mays* L. Proc. Minn. Acad. Sci. **22:** 99–104.

O'Toole, N., Hattori, M., Andres, C., Iida, K., Lurin, C., Schmitz-Linneweber, C., Sugita, M., and Small, I. (2008). On the expansion of the pentatricopeptide repeat gene family in plants. Mol. Biol. Evol. **25:** 1120–1128.

Phinney, B.O. (1956). Growth response of single-gene dwarf mutants in maize to gibberellic acid. Proc. Natl. Acad. Sci. USA **42:** 185–189.

Picardi, E., Horner, D.S., Chiara, M., Schiavon, R., Valle, G., and Pesole, G. (2010). Large-scale detection and analysis of RNA editing in grape mtDNA by RNA deep-sequencing. Nucleic Acids Res. **38:** 4755–4767.

Picardi, E., Regina, T.M., Brennicke, A., and Quagliariello, C. (2007). REDIdb: The RNA editing database. Nucleic Acids Res. **35**(Database issue): D173–D177.

Powell, L.M., Wallis, S.C., Pease, R.J., Edwards, Y.H., Knott, T.J., and Scott, J. (1987). A novel form of tissue-specific RNA processing produces apolipoprotein-B48 in intestine. Cell **50:** 831–840.

Prikryl, J., Rojas, M., Schuster, G., and Barkan, A. (2011). Mechanism of RNA stabilization and translational activation by a pentatricopeptide repeat protein. Proc. Natl. Acad. Sci. USA **108:** 415–420.

Rüdinger, M., Funk, H.T., Rensing, S.A., Maier, U.G., and Knoop, V. (2009). RNA editing: Only eleven sites are present in the *Physcomitrella patens* mitochondrial transcriptome and a universal nomenclature proposal. Mol. Genet. Genomics **281:** 473–481.

Rüdinger, M., Polsakiewicz, M., and Knoop, V. (2008). Organellar RNA editing and plant-specific extensions of pentatricopeptide repeat proteins in jungermanniid but not in marchantiid liverworts. Mol. Biol. Evol. **25:** 1405–1414.

Salmans, M.L., Chaw, S.M., Lin, C.P., Shih, A.C., Wu, Y.W., and Mulligan, R.M. (2010). Editing site analysis in a gymnosperm mitochondrial genome reveals similarities with angiosperm mitochondrial genomes. Curr. Genet. **56:** 439–446.

Salone, V., Rüdinger, M., Polsakiewicz, M., Hoffmann, B., Groth-Malonek, M., Szurek, B., Small, I., Knoop, V., and Lurin, C. (2007). A hypothesis on the identification of the editing enzyme in plant organelles. FEBS Lett. **581:** 4132–4138.

Schmittgen, T.D., and Livak, K.J. (2008). Analyzing real-time PCR data by the comparative C(T) method. Nat. Protoc. **3:** 1101–1108.

Schmitz-Linneweber, C., and Small, I. (2008). Pentatricopeptide repeat proteins: A socket set for organelle gene expression. Trends Plant Sci. **13:** 663–670.

Schmitz-Linneweber, C., Williams-Carrier, R., and Barkan, A. (2005). RNA immunoprecipitation and microarray analysis show a chloroplast pentatricopeptide repeat protein to be associated with the 5′ region of mRNAs whose translation it activates. Plant Cell **17:** 2791–2804.

Schmitz-Linneweber, C., Williams-Carrier, R.E., Williams-Voelker, P.M., Kroeger, T.S., Vichas, A., and Barkan, A. (2006). A pentatricopeptide repeat protein facilitates the trans-splicing of the maize chloroplast rps12 pre-mRNA. Plant Cell **18:** 2650–2663.

Small, I., Peeters, N., Legeai, F., and Lurin, C. (2004). Predotar: A tool for rapidly screening proteomes for N-terminal targeting sequences. Proteomics **4:** 1581–1590.

Small, I.D., and Peeters, N. (2000). The PPR motif - A TPR-related motif prevalent in plant organellar proteins. Trends Biochem. Sci. **25:** 46–47.

Steinhauser, S., Beckert, S., Capesius, I., Malek, O., and Knoop, V. (1999). Plant mitochondrial RNA editing. J. Mol. Evol. **48:** 303–312.

Steponkus, P.L., and Lanphear, F.O. (1967). Refinement of the triphenyl tetrazolium chloride method of determining cold injury. Plant Physiol. **42:** 1423–1426.

Sung, T.Y., Tseng, C.C., and Hsieh, M.H. (2010). The SLO1 PPR protein is required for RNA editing at multiple sites with similar upstream sequences in Arabidopsis mitochondria. Plant J. **63:** 499–511.

Takenaka, M. (2010). MEF9, an E-subclass pentatricopeptide repeat protein, is required for an RNA editing event in the nad7 transcript in mitochondria of Arabidopsis. Plant Physiol. **152:** 939–947.

Takenaka, M., and Brennicke, A. (2007). RNA editing in plant mitochondria: Assays and biochemical approaches. Methods Enzymol. **424:** 439–458.

Takenaka, M., and Brennicke, A. (2009). Multiplex single-base extension typing to identify nuclear genes required for RNA editing in plant organelles. Nucleic Acids Res. **37:** e13.

Takenaka, M., Verbitskiy, D., van der Merwe, J.A., Zehrmann, A., and Brennicke, A. (2008). The process of RNA editing in plant mitochondria. Mitochondrion **8:** 35–46.

Takenaka, M., Verbitskiy, D., Zehrmann, A., and Brennicke, A. (2010). Reverse genetic screening identifies five E-class PPR proteins involved in RNA editing in mitochondria of *Arabidopsis thaliana*. J. Biol. Chem. **285:** 27122–27129.

Tang, J., Kobayashi, K., Suzuki, M., Matsumoto, S., and Muranaka, T. (2010). The mitochondrial PPR protein LOVASTATIN INSENSITIVE 1 plays regulatory roles in cytosolic and plastidial isoprenoid biosynthesis through RNA editing. Plant J. **61:** 456–466.

Uchida, M., Ohtani, S., Ichinose, M., Sugita, C., and Sugita, M. (2011). The PPR-DYW proteins are required for RNA editing of rps14, cox1 and nad5 transcripts in *Physcomitrella patens* mitochondria. FEBS Lett. **585:** 2367–2371.

Vain, P., Afolabi, A.S., Worland, B., and Snape, J.W. (2003). Transgene behaviour in populations of rice plants transformed using a new dual binary vector system: pGreen/pSoup. Theor. Appl. Genet. **107:** 210–217.

van Herpen, T.W., Cankar, K., Nogueira, M., Bosch, D., Bouwmeester,

H.J., and Beekwilder, J. (2010). *Nicotiana benthamiana* as a production platform for artemisinin precursors. PLoS ONE **5:** e14222.

Verbitskiy, D., Härtel, B., Zehrmann, A., Brennicke, A., and Takenaka, M. (2011). The DYW-E-PPR protein MEF14 is required for RNA editing at site matR-1895 in mitochondria of *Arabidopsis thaliana*. FEBS Lett. **585:** 700–704.

Verbitskiy, D., Zehrmann, A., van der Merwe, J.A., Brennicke, A., and Takenaka, M. (2010). The PPR protein encoded by the LOVASTATIN INSENSITIVE 1 gene is involved in RNA editing at three sites in mitochondria of *Arabidopsis thaliana*. Plant J. **61:** 446–455.

Voinnet, O., Rivas, S., Mestre, P., and Baulcombe, D. (2003). An enhanced transient expression system in plants based on suppression of gene silencing by the p19 protein of tomato bushy stunt virus. Plant J. **33:** 949–956.

Williams, P.M., and Barkan, A. (2003). A chloroplast-localized PPR protein required for plastid ribosome accumulation. Plant J. **36:** 675–686.

Williams-Carrier, R., Kroeger, T., and Barkan, A. (2008). Sequence-specific binding of a chloroplast pentatricopeptide repeat protein to its native group II intron ligand. RNA **14:** 1930–1941.

Wittig, I., Braun, H.P., and Schägger, H. (2006). Blue native PAGE. Nat. Protoc. **1:** 418–428.

Yamato, K.T., and Newton, K.J. (1999). Heteroplasmy and homoplasmy for maize mitochondrial mutants: Isolation of a rare homoplasmic nad4 deletion plant. J. Hered. **90:** 369–373.

Yi, G., Luth, D., Goodman, T.D., Lawrence, C.J., and Becraft, P.W. (2009). High-throughput linkage analysis of Mutator insertion sites in maize. Plant J. **58:** 883–892.

Yuan, H., and Liu, D. (January 5, 2012). Functional disruption of the PPR protein SLG1 affects mitochondrial RNA editing, plant development, and responses to abiotic stresses in *Arabidopsis*. Plant J. http://dx.doi.org/10.1111/j.1365-313X.2012.04883.x.

Zapata, J.M., Salinas, C., Calderon, A.A., Munoz, R., and Barcelo, A. R. (1991). Reduction of 2,3,5-triphenyltetrazolium chloride by the Kcn-insensitive, salicylhydroxamic acid-sensitive alternative respiratory pathway of mitochondria from cultured grapevine cells. Plant Cell Rep. **10:** 579–582.

Zehrmann, A., van der Merwe, J.A., Verbitskiy, D., Brennicke, A., and Takenaka, M. (2008). Seven large variations in the extent of RNA editing in plant mitochondria between three ecotypes of *Arabidopsis thaliana*. Mitochondrion **8:** 319–327.

Zehrmann, A., Verbitskiy, D., Härtel, B., Brennicke, A., and Takenaka, M. (2011). PPR proteins network as site-specific RNA editing factors in plant organelles. RNA Biol. **8:** 67–70.

Zehrmann, A., Verbitskiy, D., van der Merwe, J.A., Brennicke, A., and Takenaka, M. (2009). A DYW domain-containing pentatricopeptide repeat protein is required for RNA editing at multiple sites in mitochondria of *Arabidopsis thaliana*. Plant Cell **21:** 558–567.

Zsigmond, L., Rigó, G., Szarka, A., Székely, G., Otvös, K., Darula, Z., Medzihradszky, K.F., Koncz, C., Koncz, Z., and Szabados, L. (2008). Arabidopsis PPR40 connects abiotic stress responses to mitochondrial electron transport. Plant Physiol. **146:** 1721–1737.